AFRL-ML-WP-TP-2007-434

FEM MODELING OF GUIDED WAVE BEHAVIOR IN INTEGRALLY STIFFENED PLATE STRUCTURES (Preprint)

Steve A. Martin and Kumar V. Jata

APRIL 2007

Approved for public release; distribution unlimited.

STINFO COPY

MATERIALS AND MANUFACTURING DIRECTORATE
AIR FORCE RESEARCH LABORATORY
AIR FORCE MATERIEL COMMAND
WRIGHT-PATTERSON AIR FORCE BASE, OH 45433-7750

REPORT DOCUMENTATION PAGE

Form Approved
OMB No. 0704-0188

1. REPORT DATE *(DD-MM-YY)*	2. REPORT TYPE	3. DATES COVERED *(From - To)*
April 2007	Conference Paper Preprint	

4. TITLE AND SUBTITLE
FEM MODELING OF GUIDED WAVE BEHAVIOR IN INTEGRALLY STIFFENED PLATE STRUCTURES (Preprint)

5a. CONTRACT NUMBER
F33615-03-C-5220

5b. GRANT NUMBER

5c. PROGRAM ELEMENT NUMBER
62102F

6. AUTHOR(S)
Steve A. Martin (NDE Computational Consultants)
Kumar V. Jata (Nondestructive Evaluation Branch (AFRL/MLLP))

5d. PROJECT NUMBER
4349

5e. TASK NUMBER
41

5f. WORK UNIT NUMBER
43494108

7. PERFORMING ORGANIZATION NAME(S) AND ADDRESS(ES)

Nondestructive Evaluation Branch (AFRL/MLLP)
Metals, Ceramics, and Nondestructive Evaluation Division
Materials and Manufacturing Directorate
Air Force Research Laboratory, Air Force Materiel Command
Wright-Patterson Air Force Base, OH 45433-7750

NDE Computational Consultants
7697 Aldridge Place
Dublin, OH 43017

8. PERFORMING ORGANIZATION REPORT NUMBER
AFRL-ML-WP-TP-2007-434

9. SPONSORING/MONITORING AGENCY NAME(S) AND ADDRESS(ES)
Materials and Manufacturing Directorate
Air Force Research Laboratory
Air Force Materiel Command
Wright-Patterson AFB, OH 45433-7750

10. SPONSORING/MONITORING AGENCY ACRONYM(S)
AFRL-ML-WP

11. SPONSORING/MONITORING AGENCY REPORT NUMBER(S)
AFRL-ML-WP-TP-2007-434

12. DISTRIBUTION/AVAILABILITY STATEMENT
Approved for public release; distribution is unlimited.

13. SUPPLEMENTARY NOTES
PAO Case Number: AFRL/WS 07-0091, 20 March 2007. To be presented at the 14th International Symposium on Smart Structures and Materials and Nondestructive Evaluation and Health Monitoring, 18 March 2007, San Diego, CA. The U.S. Government is joint author of this work and has the right to use, modify, reproduce, release, perform, display, or disclose the work.

14. ABSTRACT
Structural health monitoring (SHM) technologies, which use integrated sensing for damage detection, are expected to improve system reliability, availability, and operational cost. Guided waves can propagate great distances while experiencing low attenuation. They have been successfully used for damage detection in structures of relatively low geometric complexity such as plates and cylindrical pipes. The use of guided waves for this purpose becomes increasingly difficult as the geometric complexity of the structure increases. Aerospace structural components such as fuel tanks, wings, etc. often are comprised of substructures that consist of plates with integral stiffeners. This work reports on finite element simulations of guided waves in integrally stiffened plate structures. In these studies, the guided waves are generated by PZT wafer-type transducers mounted on the structure. Transient dynamic finite element simulations using PZFlex, in 2D and in 3D, were used to model both the structure and transducers. The interaction of the guided waves with cracks, simulated by notches of varying dimensions, is also modeled. This allows appraisal of the sensitivity of various modes for crack detection by providing insight into mode conversion and scattering resulting from the guided wave and crack interaction.

15. SUBJECT TERMS

16. SECURITY CLASSIFICATION OF:			17. LIMITATION OF ABSTRACT:	18. NUMBER OF PAGES	19a. NAME OF RESPONSIBLE PERSON (Monitor)
a. REPORT	b. ABSTRACT	c. THIS PAGE			Kumar V. Jata
Unclassified	Unclassified	Unclassified	SAR	18	19b. TELEPHONE NUMBER *(Include Area Code)* (937) 255-9802

Standard Form 298 (Rev. 8-98)
Prescribed by ANSI Std. Z39-18

FEM Modeling of Guided Wave Behavior in Integrally Stiffened Plate Structures

Steven A. Martin[*b] and Kumar V. Jata[a]
[a]Air Force Research Laboratory, MLLP, NDE Branch,
Wright Patterson Air Force Base, Dayton, OH, OH 45433;
[b]NDE Computational Consultants, 7697 Aldridge Place, Dublin, OH, USA 43017

ABSTRACT

Structural health monitoring (SHM) technologies, which use integrated sensing for damage detection, are expected to improve system reliability, availability, and operational cost. Guided waves can propagate great distances while experiencing low attenuation. They have been successfully used for damage detection in structures of relatively low geometric complexity such as plates and cylindrical pipes. The use of guided waves for this purpose becomes increasingly difficult as the geometric complexity of the structure increases. Aerospace structural components such as fuel tanks, wings, etc. often are comprised of substructures that consist of plates with integral stiffeners. This work reports on finite element simulations of guided waves in integrally stiffened plate structures. In these studies, the guided waves are generated by PZT wafer-type transducers mounted on the structure. Transient dynamic finite element simulations using PZFlex, in 2D and in 3D, were used to model both the structure and transducers. The interaction of the guided waves with cracks, simulated by notches of varying dimensions, is also modeled. This allows appraisal of the sensitivity of various modes for crack detection by providing insight into mode conversion and scattering resulting from the guided wave and crack interaction.

Keywords: **Keywords:** Finite element simulation, integrally stiffened plate, ultrasonics, bonded transducer, Structural Health Monitoring

1. INTRODUCTION

Structural Health Monitoring (SHM) has the functional goals of determining when, where, and to what extent structural damage has occurred through the use of integrated sensing. A possible further functional objective is the sensing of precursors to damage. The driving operational forces behind the developing field of Structural Health Monitoring (SHM) are the goals of increasing system reliability, improving system availability, and reducing inspection and maintenance costs. The use of integrated ultrasonic transducers and guided waves is a technology that is viewed as having great potential for SHM.

Guided waves have the ability to cover a large region of a structure from a transducer or group of transducers resident in a small area. Much of the research and implementation performed to date has focused on inspection of plate and tubular structures[1]. This is reasonable in view of the relatively low geometric complexity of these structures. Another area that has received considerable attention is multilayer structures. Lap joints and ‘doublers’ are examples of typical aerospace applications[2].

An integrally stiffened structure results when a plate has a stiffener attached, usually at a right angle to the plate surfaces. The simplest example of this geometry is the extruded T-Section. The cross section of this geometry is illustrated in Figure 1. They represent a somewhat greater geometric complexity than plate, tube, and multilayer structures. Integrally stiffened structures have many applications in aerospace vehicles. They commonly appear as substructures in wings, airframes, and fuel tanks.

*steven.martin@wpafb.af.mil; phone 1 937-255-7239; fax 1 937-255-9804

Coupling of Lamb modes at a T junction was experimentally investigated by Morvan, et al.[3]. Greve, et al. reported on a numerical simulation of Lamb wave propagation in a plate girder("I-Beam") geometry[4]. This simulation had an S_0 Lamb wave generated in the web and studied the interaction of the S_0 mode with a crack in the weld bead on the web side of the web-flange interface. A two-dimensional T-Section geometry with fillets with and without notch defects is numerically simulated by Aldrin, et al.[5].

The objective of this study is to investigate the generation and interaction of guided waves in a three dimensional T-section geometry both with and without notches to simulate cracks. The waves are generated in the base of the T-Section, which would correspond to a girder flange. This modeling includes an explicit model of a bonded transducer disk to more closely simulate experimental observation and also allow observation of the three dimensional effects.

2. FINITE ELEMENT MODEL

In this work we examine the two dimensional and three dimensional T-Section problems. The 2D geometry corresponding to the 3D cross-sectional geometry is shown in Figure 1. The model is geometrically parameterized in terms of the thickness and length of the left leg, thickness and length of the vertical leg, thickness and length of the right leg, and the extrusion width. The bonded transducer is also parameterized in terms of the transducer radius and thickness. The transducer location is parameterized in terms of offsets from the symmetry planes of the 3D T-Section. There are also validity checks which keep the sensor inside the bounds of the part and do not allow placement too close to the vertical leg. The parameter values of the model for this study are: t_1 = 2.21 mm, t_2 =2.21 mm, t_3 =2.21 mm, t_t = 0.19 mm, w_1 =30.0 mm, w_2 = 90.0 mm, w_3 = 12.7 mm, w_t =80.0 mm, and r_t = 5.0 mm.

The 3D geometry of the model showing the transducer and the length, d = 30.0 mm, in the extrusion direction is shown in Figure 2. The transducer disk bonded to the top side, centered on the extrusion dimension symmetry plane, of the plate is made of PZT-5H. The transducer electrodes are on its top surface and bottom surface. The signal is applied at the top surface with the bottom surface being grounded. The interface between the transducer and the structure is modeled as being 'welded', i.e. the adhesive layer is not explicitly modeled and the displacement and force are continuous across the interface. The piezoelectric equations are solved within a volume of a rectangular parallelepiped ('electric window') whose dimensions are equal to the diameter and thickness of the transducer. The crack location is also shown in Figure 1. The notches at the base were all 0.29mm wide(longitudinal direction). Three notch depths(transverse direction) were modeled in addition to the notch free configuration. The notch depths, t_n, were 0.402, 0.804, and 1.206 mm. The notches in the 3D model ran across the entire extrusion depth, 30 mm.

The voltage applied to the transducer in the model uses a single cycle sine function at a frequency of 500MHz. The signal is 10 volts peak to peak. The outer planes have an absorbing boundary condition applied. This removes the complications of reflected signals and the model can be viewed as a piece of a much larger structure. The f·d product is 1.11 mm·MHz and is in the region of the Lamb wave dispersion curve where only the A_0 and S_0 modes are expected to be present[6-7]. The mesh density in the model was approximately 60 elements per wavelength at 500 MHz. This model was generated and run using the PZFlex Finite Element software[8].

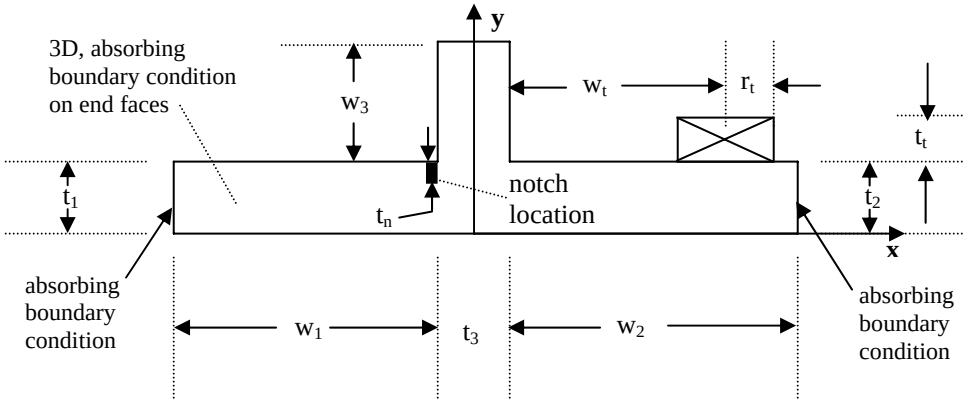

Fig. 1. Diagram of a T-section (Integrally Stiffened Plate) showing transducer and notch location.

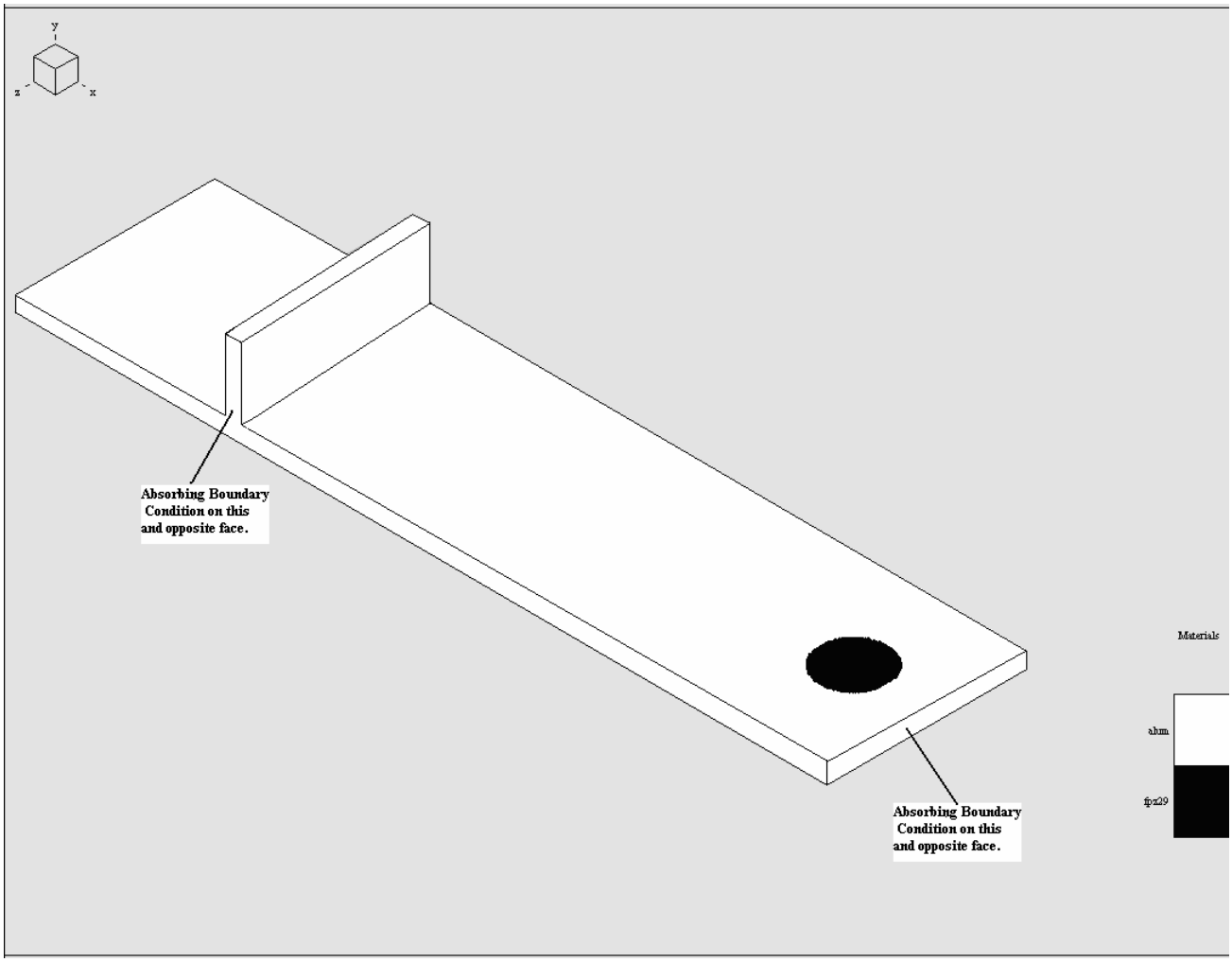

Fig. 2. Three Dimensional T-section (Integrally Stiffened Plate) showing extrusion depth and transducer and location.

3. DISCUSSION OF RESULTS

The response of the 2D and 3D T-Sections to the transducer input, both without and with notches, were run for this study. The stresses displayed in the figures are the difference between the normal stresses in the directions parallel, x, and orthogonal, y, to the centerline of the bottom plate. This stress is what is observed in photoelastic wave visualization experiments[9]. The terminology of 'photoelastic' stress is adopted for this paper. This can be expressed as:

$$\sigma_p = \sigma_{yy} - \sigma_{xx} \tag{1}$$

where σ_p is the photoelastic stress, σ_{yy} is the y normal stress, and σ_{xx} is the x normal stress. These stresses are calculated through the use of the scripting environment available in PZFlex which allows access to the data structures which contain the native field variables that the software does calculate.

3.1 2D Model

The photoelastic stress, for the un-notched 2D model, is shown in Figure 3 for a time shortly after the wave front of the response has encountered the T junction. This figure contains vertical bands on the left hand side which are indicative of the S_0 mode. The S_0 mode has a higher propagation velocity than the A_0 mode and is separating out of the mixture of the two modes generated by the transducer pulse. The patterns closer to the transducer have vertical bands which change sign but at a point away from the centerline. This indicates a mixture of both A_0 and S_0 modes. The bottom view in the figure is a close-up of the T junction. The interesting phenomenon observed in this view is that the pattern induced in the vertical stiffener appears to be indicative of an A_0 mode even though only excitation is the 'pure' S_0 wave front. A possible explanation for this is that the S0 wave, of frequency f, passing by the stiffener excites it at that frequency f. Since the wave is approximately sinusoidal in the thickness direction the excitation will consist of spatially symmetric and anti-symmetric portions. The stiffener thickness is the same as base plate thickness which results in the same fd value as the base plate.

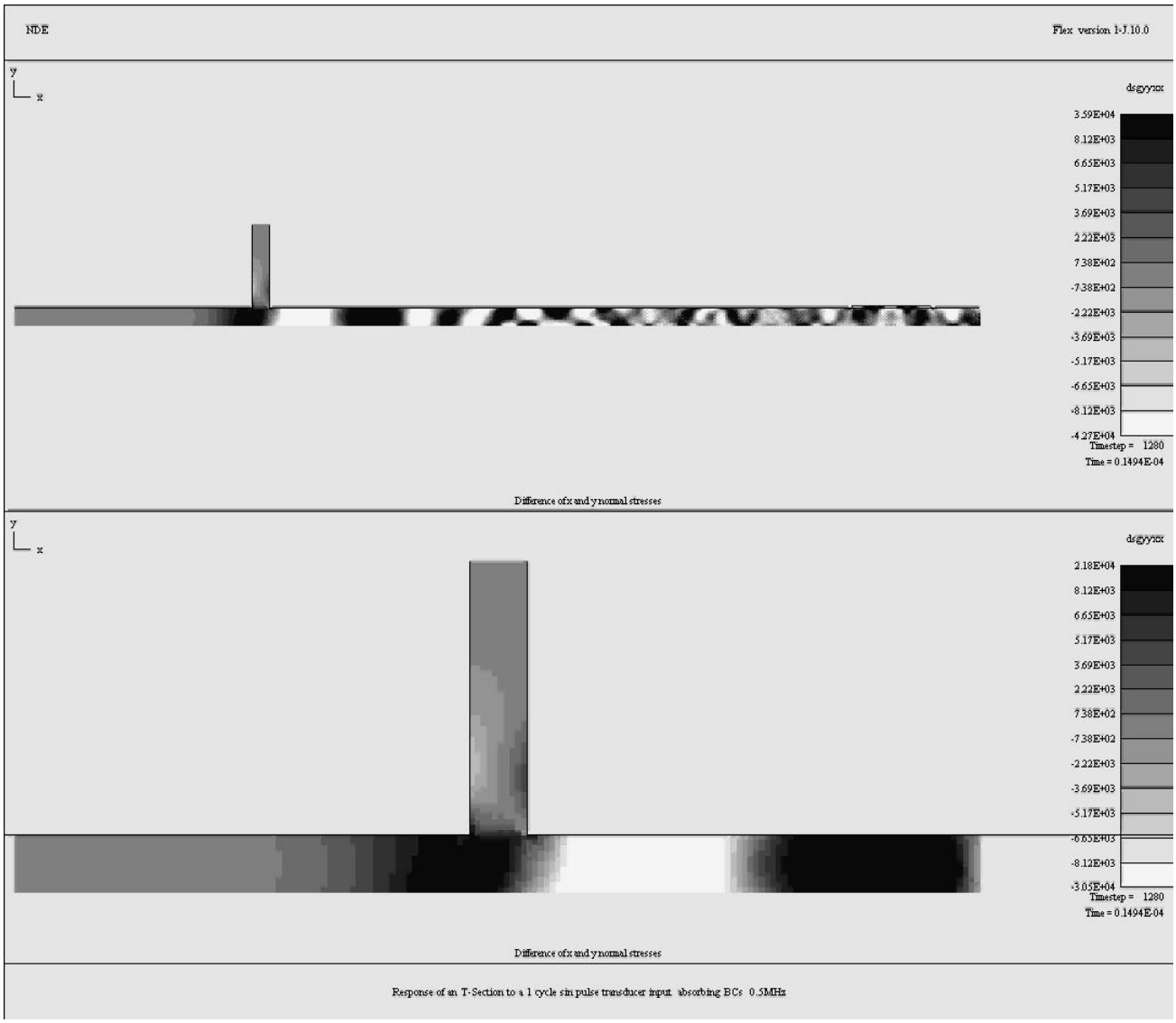

Fig. 3. Photoelastic stress, Pa, response of a 2D T-section to a single cycle sine pulse transducer input at time = 14.94 μs.

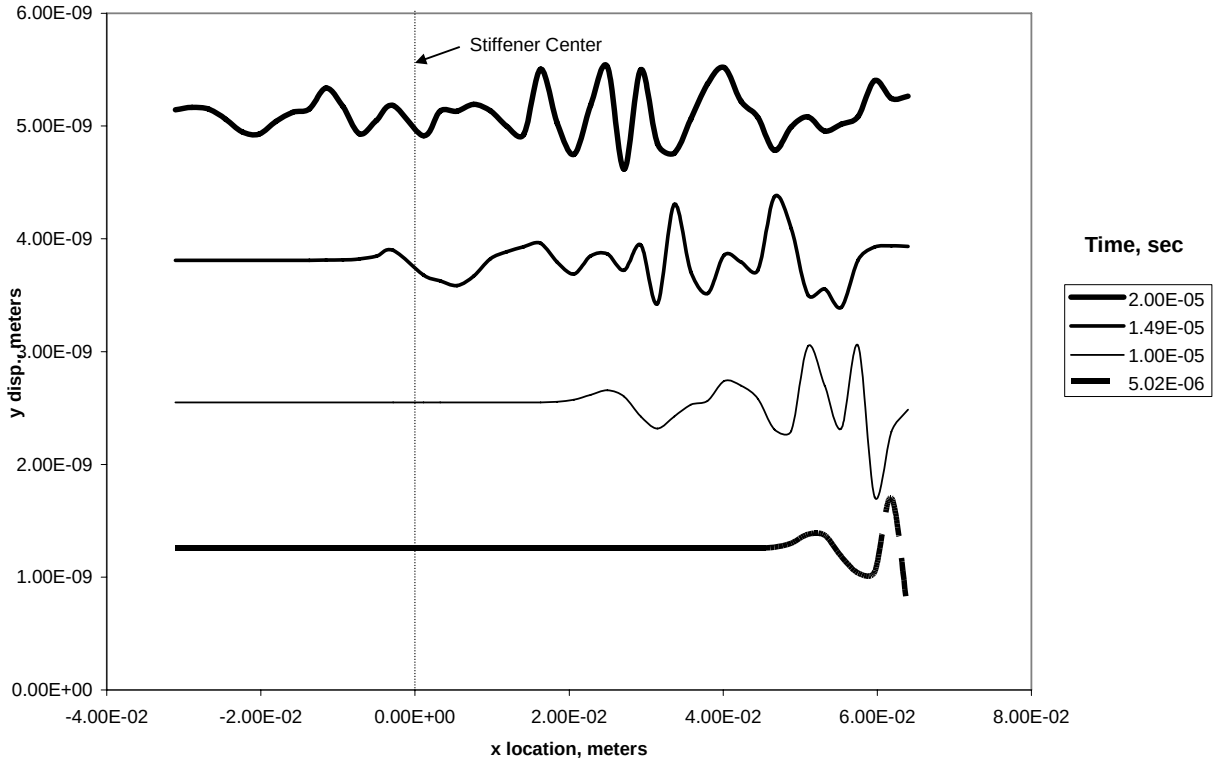

Fig. 4. y displacement profiles at various times along top of plate for a 2D T-section subjected to a single cycle sine pulse transducer input.

The transverse, y, displacements along the top of the plate on the center cross-section at various times are shown in Figure 4. These show the S_0 modes separating from the A_0 modes as time progresses. The plot for 14.9 μs (1.49 e-05 seconds) corresponds to the photoelastic stress plot in Figure 3. The differences in the baseline (i.e. un-notched) and notched cases are difficult to differentiate visually. Figure 5 is a plot of the y displacement at various x locations on top of the plate. The propagation of the wave front through the structure may be clearly seen. Figure 6 is a plot of the differential signal between the baseline and notched y displacement at various x locations on top of the plate. The differential signal is observed to originate at the notch location and propagate out in both directions. The differential signals of the three different notch sizes received at the x location value of -235 mm are shown in Figure 7. These signals appear to increase in magnitude and experience an increasingly lagging phase shift with increasing notch depth. This could be the result the reduction in plate thickness causing a shift along the dispersion curve in the notch region. Further investigation of this is desirable.

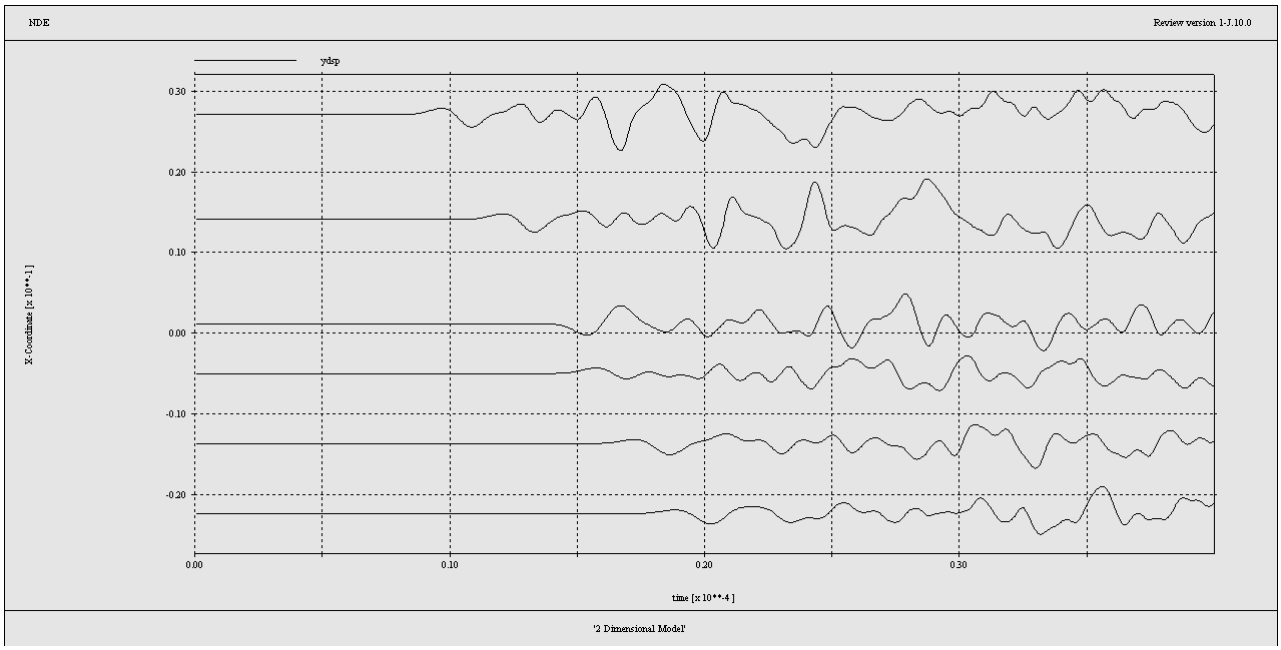

Fig. 5. y displacement versus time on top of plate at various x locations for a 2D T-section subjected to a single cycle sine pulse transducer input.

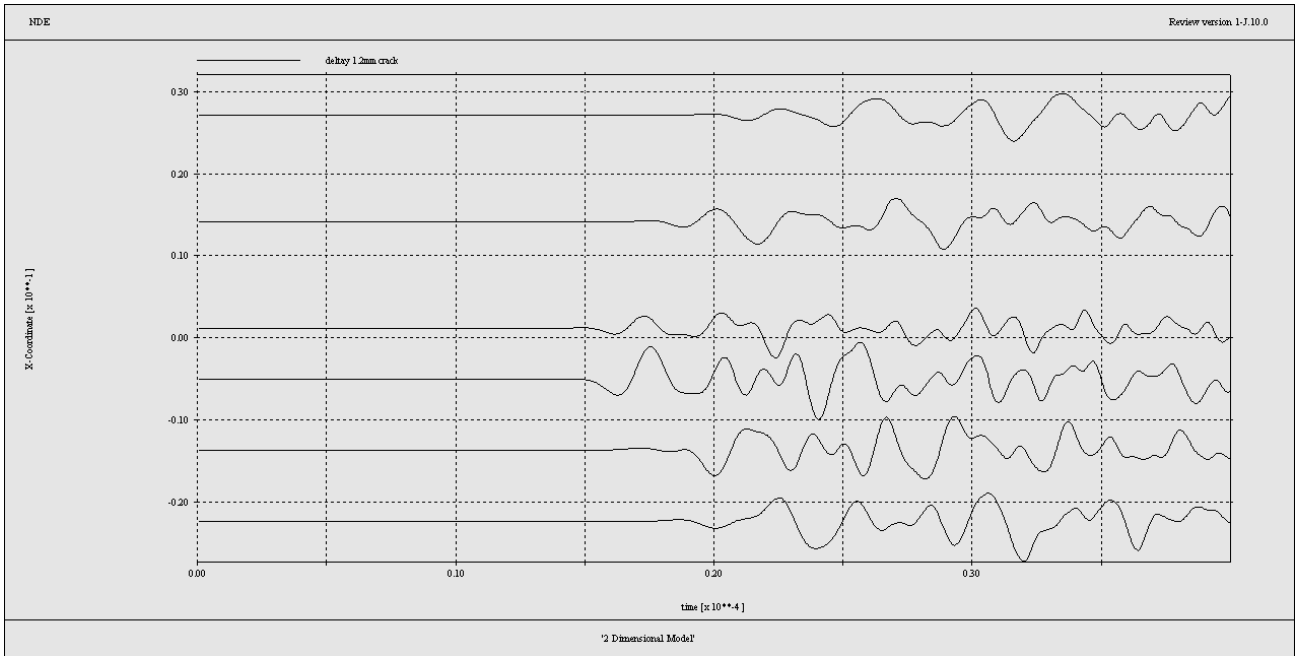

Fig. 6. Differential y displacement comparing base and 1.2 mm cases versus time on top of plate at various x locations for a 2D T-section subjected to a single cycle sine pulse transducer input.

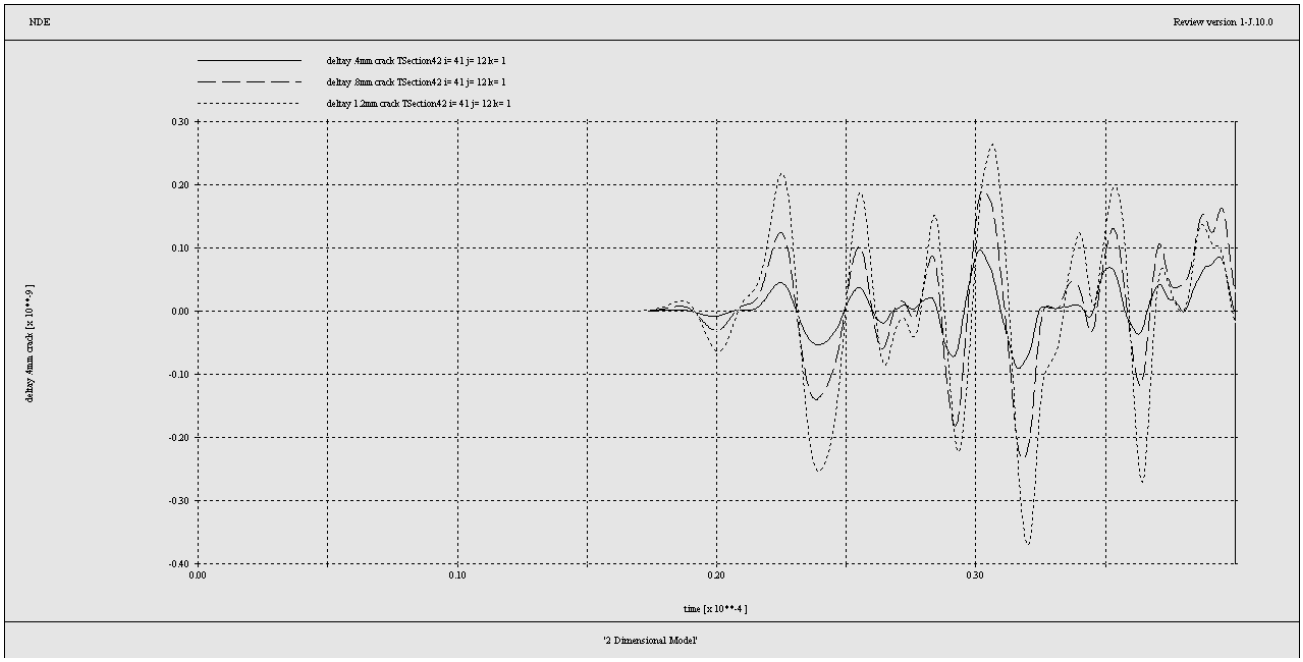

Fig. 7. Differential y displacement of 0.4 mm, 0.8 mm, 1.2 mm and base cases versus time on top of plate at x location -235 mm for a 2D T-section subjected to a single cycle sine pulse transducer input.

3.2 3D Model

Figure 8 shows the photoelastic stresses along cross sections of the 3D geometry. The cross sections are taken normal to the 'extrusion' direction of the T-section. There are five cross sections, taken in equal increments, starting at the center of the T-section and ending at the outer edge. Since the model is symmetric, only half of the model is shown. The sub-windows show close-ups of the T junction where the vertical stiffener meets the base plate. These start at the center and move outward in equal increments toward the edge. A close-up of the outer boundary is not shown.

The character of the response, especially along the center cross section of the model, displays great similarity to the 2D case. The transducer in the 3D model is a circular disk. The axisymmetry of the transducer geometry gives the expectation that circular crested Lamb waves[10] will be generated instead of the straight crested Lamb waves that result in the two dimensional plane strain case. Circular crested waves have displacement functions through the thickness that are similar to the straight crested case but they are weighted by Bessel functions in the radial direction. The wave lengths are also functions of the radial coordinate but asymptotically approach the straight crested case. In addition, the straight crested dispersion curves also display great similarity to the circular crested case. The subsequent discussion of S_0 and A_0 modes refers to the circular crested equivalents of the straight crested Lamb modes. Figure 8 indicates a mixture of A_0 and S_0 modes analogous to the 2D situation. The close-up of the 3D T junction also displays an A_0 type pattern induced in the vertical stiffener even though it has only experienced excitation by a 'pure' S_0 wave front.

Figure 9 displays the transverse, y, displacements along the top of the plate on the center cross-section at various times. The S_0 modes appear to separate from the A_0 modes as time progresses. The plot for 1.49 e-05 seconds is close to the 1.64e-05 seconds of the photoelastic stress plot in Figure 8. A plot of the y displacement at various x locations on top of the plate is shown in Figure 10. The wave front propagation through the structure is clearly shown. The difference between the un-notched (base) and the notched cases is hard to detect visually. A plot of the differential signal between the baseline and notched y displacement at various x locations on top of the plate is illustrated in Figure 11. As in the 2D situation, the differential signal is observed to originate at the notch location and propagate out in both directions. The differential signals resulting from the three different notch sizes received at the x location value of -235 mm are shown in Figure 12. These signals appear to increase in magnitude and experience an increasing phase shift with increasing notch depth in a manner analogous to that observed in 2D. Comparison of Figures 4 and 9 shows the greater attenuation of the 3D guided waves. This attenuation is also evidenced by the greater magnitude of the 2D differential signal in Figure 7 versus the 3D signal in Figure 12.

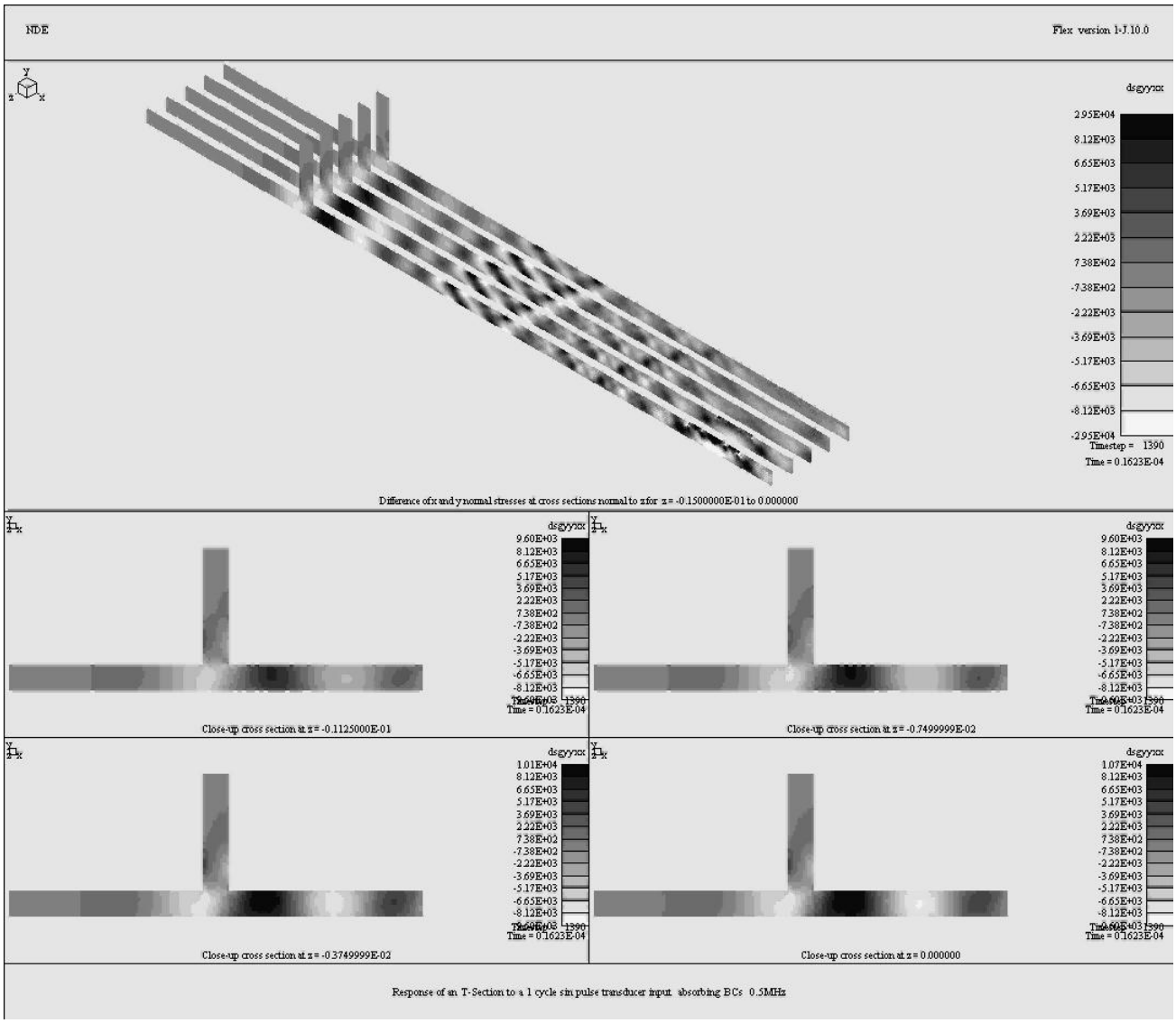

Fig. 8. Photoelastic stress, Pa, response of a 3D T-section to a single cycle sine pulse transducer input at time = 16.23 μs.

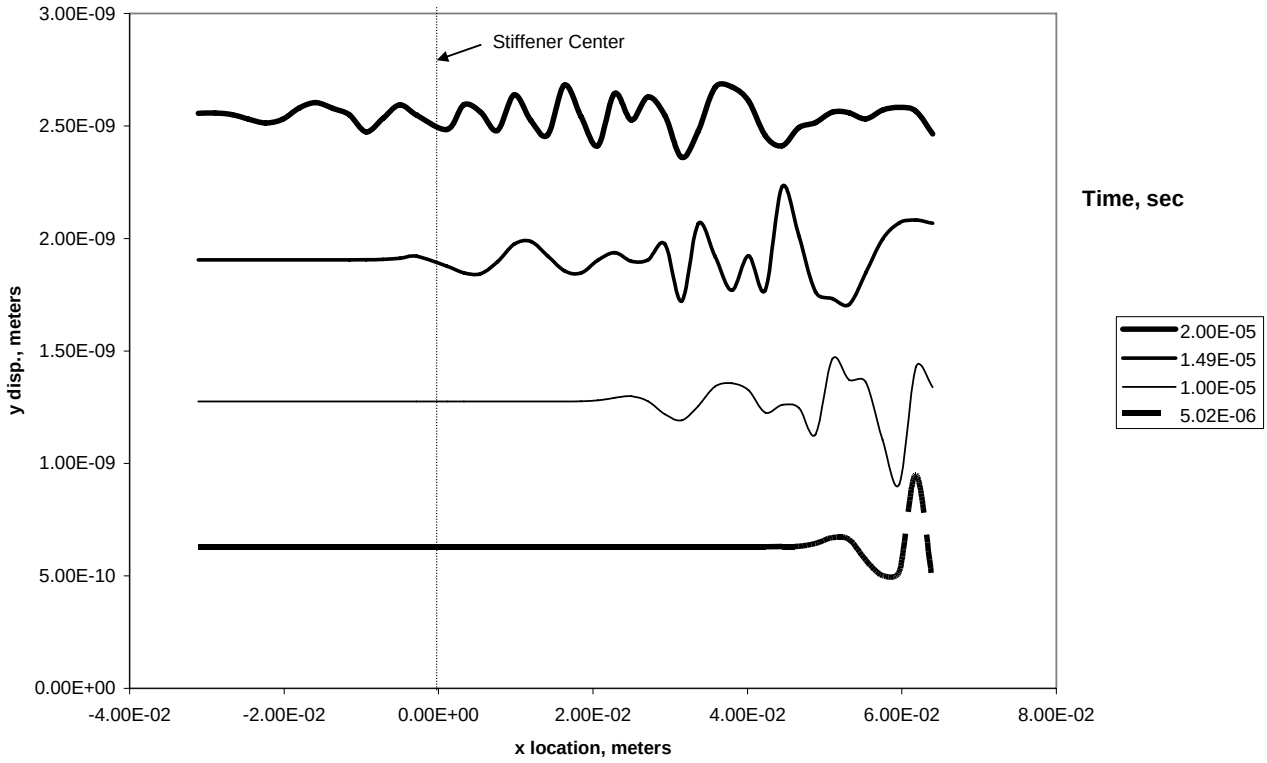

Fig. 9. y displacement profiles at various times along top of plate for a 3D T-section subjected to a single cycle sine pulse transducer input.

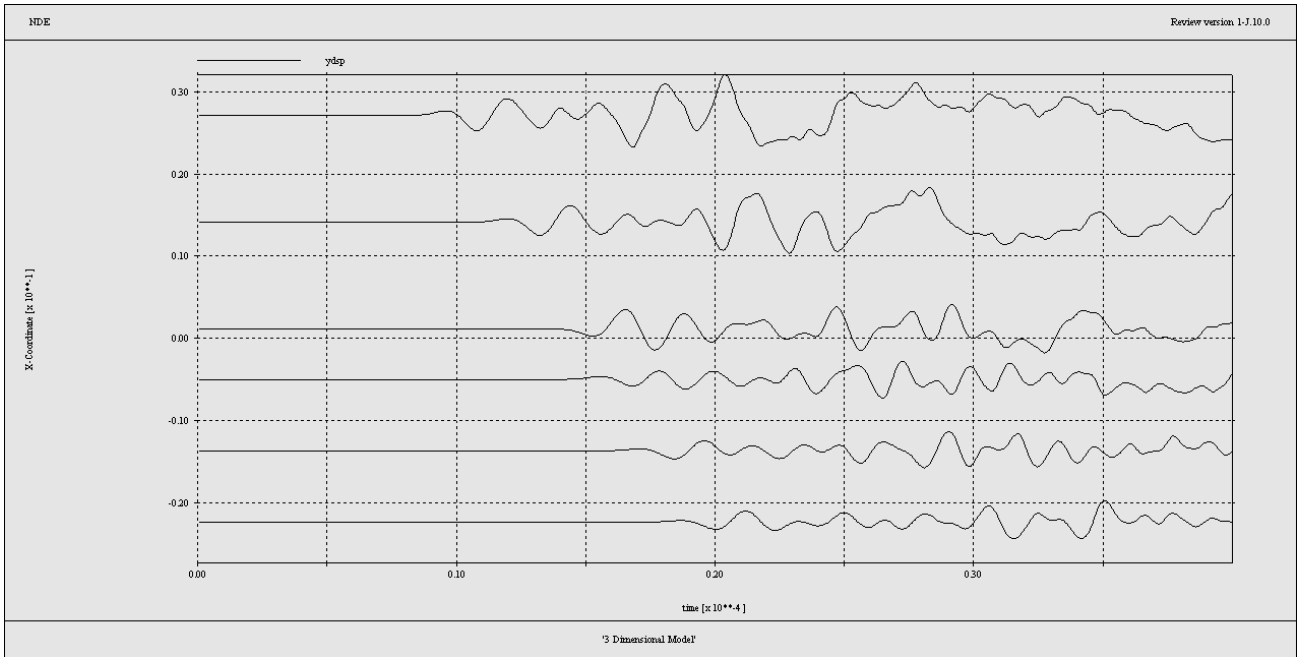

Fig. 10. y displacement versus time on top of plate at various x locations for a 3D T-section subjected to a single cycle sine pulse transducer input.

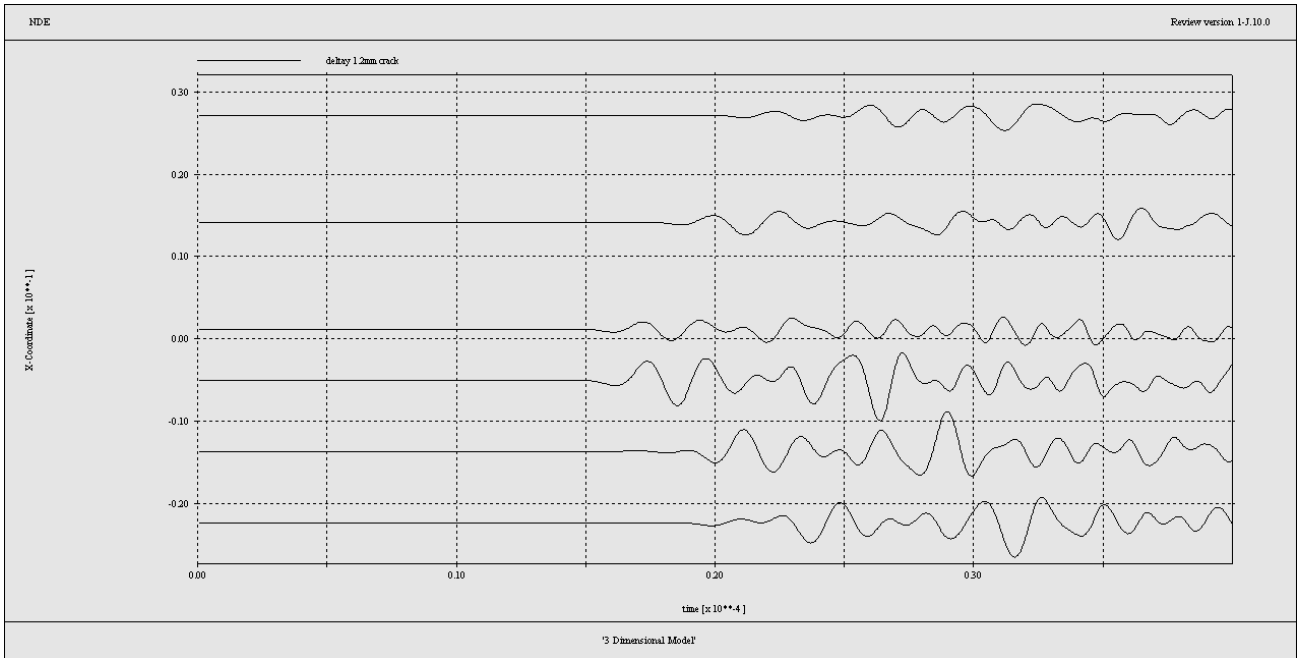

Fig. 11. Differential y displacement comparing base and 1.2 mm cases versus time on top of plate at various x locations for a 3D T-section subjected to a single cycle sine pulse transducer input.

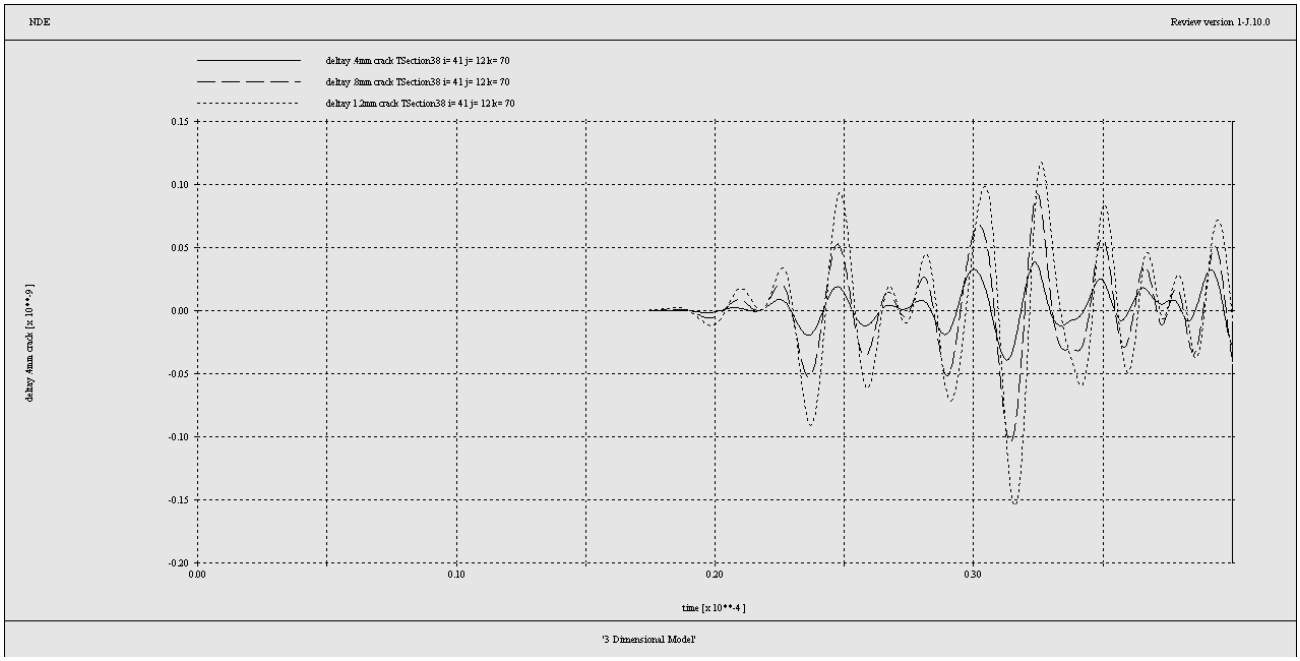

Fig. 12. Differential y displacement of 0.4 mm, 0.8 mm, 1.2 mm and base cases versus time on top of plate at x location -235 mm for a 3D T-section subjected to a single cycle sine pulse transducer input.

4. CONCLUSIONS

The response of a 2D and 3D integrally stiffened geometry with and without notching to excitation by a piezoelectric transducer was modeled by using Finite Element analysis. The response along the center section of the 3D structure to a circular disk transducer is quite similar in character to the 2D model excited by a strip transducer. In comparison to the straight crested Lamb waves generated in the 2D case, the circular crested Lamb waves of the 3D case do attenuate in perfectly elastic material due to spreading. This does not present a problem if the distances involved are not great but large enough that the waves have asymptotically approached straight crested behavior. Both models had the appropriate S0 and A_0 modes generated. Separation between the two modal types was observed as propagation progressed due to their different velocities.

The change in response to the excitation due to different sized notches at the base of the T junction was also modeled. The comparison is done with the baseline (un-notched) case. There is a differential observed in the displacements along the centerline of the top of the plate in the signals received with and without the notch present. These differential signals display magnitudes and phase shifts that scale with increasing notch size.

Several possibilities present themselves as areas for future work. A comparison with experimental observation is desirable. A study of the case where a receiving transducer is explicitly modeled and the size of notch required for detection would further tie this work to actual practice. Another valuable investigation is the effect of the stiffener geometry on the mode conversion and the effect of reflection from the top surface of the stiffener back into the base plate.

5. ACKNOWLEDGEMENTS

This work is supported by the U.S. Air Force research laboratory, Nondestructive Evaluation Branch, thru United States Air Force Contract F33615-03-C5220.

REFERENCES

1. J. L. Rose, *Ultrasonic Waves in Solid Media*, Cambridge University Press, New York, NY, 1999.
2. S. I. Rohklin, “Lamb wave interaction with lap-shear adhesive joints: Theory and experiment,” *J. Acoust. Soc. Am.*, Vol. 89(6), pp. 2758-2765, 1991.
3. B. Morvan, A. Tinel, and J. Duclos, "Coupling of Lamb modes at a tee junction," *IEEE Ultrasonics Symposium*, pp. 565-568, 1999.
4. D. W. Greve, N. Tyson, and I.J. Oppenheim, "Interaction of defects with Lamb waves in complex geometries," *IEEE Ultrasonics Symposium*, pp. 297-300, 2005.
5. J. C. Aldrin, E. A. Medina, K. V. Jata, J. S. Knopp, “Simulation-Based Design of a Guided-Wave Structural Health Monitoring System for a Plate-Stiffener Configuration”, *Proceedings of the 3rd European Workshop on Structural Health Monitoring*, pp. 1078-1085, 2006.
6. B. A. Auld, *Acoustic Fields and Waves in Solids*, Krieger Publishing Co., Malabar, FL, Vol. II, pp. 76-88, 1973.
7. V. Giurgiutiu, "Lamb Wave Generation with Piezoelectric Wafer Active Sensors for Structural Health Monitoring," *Proceedings of SPIE Smart Materials and Structures*, 5056, pp. 111-122, 2003.
8. PZFLEX, *Flex User’s Manual*, Weidlinger Associates, Los Altos, CA, 2005, http://www.pzflex.com
9. H. U. Li and K. Negishi, "Visualization of Lamb mode patterns in a glass plate," *Ultrasonics* 32(4), pp. 243-248, 1994.
10. L. E. Goodman, "Circular-crested vibrations of an elastic solid bounded by two parallel planes," *Proc. Ist Natn. Congr. Appl. Mech.*, pp. 65-73, ASME, New York, 1952.